Genomics **72,** 285–296 (2001)
doi:10.1006/geno.2000.6456, available online at http://www.idealibrary.com on IDEAL®

Myosin-VIIb, a Novel Unconventional Myosin, Is a Constituent of Microvilli in Transporting Epithelia

Zheng-Yi Chen,*,[1] Tama Hasson,† Duan-Sun Zhang,*,‡ Brian J. Schwender,*,‡ Bruce H. Derfler,*,‡ Mark S. Mooseker,§ and David P. Corey*,‡,[1]

‡*Howard Hughes Medical Institute,* **Department of Neurology and Department of Neurobiology, Massachusetts General Hospital and Harvard Medical School, Boston, Massachusetts 02114; †Division of Biology, University of California at San Diego, La Jolla, California 92093; and §Department of MCD-Biology, Department of Cell Biology, and Department of Pathology, Yale University, New Haven, Connecticut 06520*

Received September 5, 2000; accepted November 23, 2000

Mouse myosin-VIIb, a novel unconventional myosin, was cloned from the inner ear and kidney. The human myosin-VIIb (HGMW-approved symbol MYO7B) sequence and exon structure were then deduced from a human BAC clone. The mouse gene was mapped to chromosome 18, approximately 0.5 cM proximal to D18Mit12. The human gene location at 2q21.1 was deduced from the map location of the BAC and confirmed by fluorescence *in situ* hybridization. Myosin-VIIb has a conserved myosin head domain, five IQ domains, two MyTH4 domains coupled to two FERM domains, and an SH3 domain. A phylogenetic analysis based on the MyTH4 domains suggests that the coupled MyTH and FERM domains were duplicated in myosin evolution before separation into different classes. Myosin-VIIb is expressed primarily in kidney and intestine, as shown by Northern and immunoblot analyses. An antibody to myosin-VIIb labeled proximal tubule cells of the kidney and enterocytes of the intestine, specifically the distal tips of apical microvilli on these transporting epithelial cells.

INTRODUCTION

Myosins constitute a large gene family of motor proteins that bind and move along actin filaments using mechanical energy derived from ATP hydrolysis. Seventeen classes of myosins (>40 myosin genes) have been identified in various species, eight of them in vertebrates. All myosins have a conserved head domain which binds actin and hydrolyzes ATP; in nearly all myosins this is followed by a neck region with one to six copies of a regulatory light-chain-binding element (IQ motif). The tails of myosins are considerably more divergent, presumably reflecting the specificity of different myosins for different kinds of cargo proteins. However, some elements thought to be protein-binding domains, such as SH3, MyTH4, and FERM domains, appear in the tails of myosins of many different myosin classes (Chen *et al.*, 1996; Kuriyan and Cowburn, 1997; Oliver *et al.*, 1999; Wu *et al.*, 2000). Phylogenetic relationships among myosins have been determined from sequences of the conserved head domains, but conserved elements of the tail may offer additional insight into myosin evolution.

Mutations in certain myosins cause disease in mice and humans. Familial hypertrophic cardiomyopathy arises from mutations in a cardiac type II myosin (Geisterfer-Lowrance *et al.*, 1990). Myosin-Va is mutated in the mouse *dilute* mutant (Mercer *et al.*, 1991) and in the human Griscelli–Prunieras syndrome, a lethal disease combining immunodeficiency with neurologic and pigment dilution (Pastural *et al.*, 1997). Mutations in myosins-VI, -VIIa, and -XV cause congenital deafness and vestibular disorders: The myosin-VI gene is rearranged or truncated in alleles of the deaf mouse mutant *Snell's waltzer* (*sv*) (Avraham *et al.*, 1995). Myosin-VIIa is defective in Usher syndrome type Ib, the most common blindness–deafness syndrome in humans, and in two nonsyndromic deafnesses—DFNB2 and DFNA11 (Weil *et al.*, 1995; Liu *et al.*, 1997; Weil *et al.*, 1996). In mouse, myosin-VIIa is also mutated in the *shaker-1* (*sh1*) deafness mutant (Gibson *et al.*, 1995). A new class of myosin, myosin-XV, is defective in the human nonsyndromic deafness DFNB3 and in the deaf mouse *shaker-2* (*sh2*) (Probst *et al.*, 1998; Wang *et al.*, 1998; Liang *et al.*, 1999).

A few lines of evidence suggest that there may be additional genes related to myosin-VIIa. Bement *et al.* (1994) cloned a 130-bp cDNA fragment from a human intestinal epithelium cell line, which was most similar to myosin-VIIa. This human fragment was mapped to two different locations in the mouse genome, neither

Sequence data from this article have been deposited with the EMBL/GenBank Data Libraries under Accession Nos. AF242411 and AC010976.

[1] To whom correspondence should be addressed at Department of Neurobiology, WEL414, Massachusetts General Hospital, Boston, MA 02114. Telephone: (617) 726-6147. Fax: (617) 726-5256. E-mail: corey@helix.mgh.harvard.edu.

0888-7543/01 $35.00

corresponding to the location of myosin VIIa (Hasson *et al.*, 1996). Moreover, defects in myosin-VIIa cause progressive blindness in human but not in mouse, suggesting that a related myosin may substitute for myosin-VIIa in mouse retina (Gibson *et al.*, 1995; Weil *et al.*, 1996).

We report here the cloning of mouse myosin-VIIb, a homologue of myosin-VIIa. Mapping of myosin-VIIb in mouse and human reveals a new region of homologous synteny. The exon structure of human myosin-VIIb[2] has been inferred from the mouse cDNA and a human BAC sequence. The domain structure of myosin-VIIb is very similar to that of myosin-VIIa, but it lacks a coiled-coil domain, suggesting differences in function. Antibodies to myosin-VIIb strongly label the microvilli of intestinal and kidney brush border, indicating a role in the apical membranes of transporting epithelia.

MATERIALS AND METHODS

Cloning. Based on the sequence of the 130-bp human cDNA fragment previously isolated (Accession No. I61698; Bement *et al.*, 1994), we designed two upstream PCR primers (my7b-1for, 5′-GAGACCACCAAGCTCATCCTG-3′; and my7b-4for, 5′-GTCCTG-GAAGCCAACCCCATC-3′). One downstream degenerate primer (NEK, 5′-TA(T/C)CT(G/T)(C/T)T(C/G/T)GA(G/A)AA(A/G)TC-3′) was derived from a highly conserved region of myosin heads that usually includes the amino acid sequence NEKLQQ (Solc *et al.*, 1994). Semi-nested RT-PCR was performed with my7b-1for/NEK followed by my7b-4for/NEK, using AmpliTaq (Perkin–Elmer) and cDNA prepared from mouse utricle (Chen *et al.*, 1996). The product of about 850 nucleotides representing the middle of the head domain was subcloned into the TA-cloning vector pCR2.1 (Clontech).

We then found two mouse ESTs that were similar but not identical to mouse myosin-VIIa (W15882 and AA109944; Fig. 1); these were obtained from Research Genetics and sequenced in full. Reasoning that these might represent myosin-VIIb, we performed RT-PCR between them using primers designed to produce overlapping fragments (Fig. 1). Because Northern analysis revealed a high level of expression in kidney, we used cDNA prepared from mouse kidney. To obtain the 5′ end of the coding sequence, RACE was performed using Marathon-Ready mouse kidney cDNA (Clontech). RACE–PCR fragments were cloned into the TA-cloning vector as described as above. The sequence has been deposited with GenBank under Accession No. AF242411.

Genomic structure of human myosin-VIIb. Two human BAC sequences in the High Throughput Genomic Sequences database (Accession Nos. AC010976 and AC010898) were found to contain a high degree of sequence similarity to mouse myosin-VIIb. The exon structure for human myosin-VIIb was inferred by comparing the BAC sequence to the mouse cDNA sequence and searching for splice donor and acceptor sites.

Mapping of myosin-VIIb in human and mouse. Mouse myosin-VIIb was mapped using the genomic DNA provided by The Jackson Laboratory Backcross DNA Panel Mapping Resource's interspecific backcross panels (C57BL/6J × *Mus spretus*) xC57BL/6J(BSS) and (C57BL/6JEi x SPRET/Ei)F1 x SPRET/Ei (BSB) (Rowe *et al.*, 1994). A PCR-based assay was performed using mouse myosin-VIIb-specific primers (myo7b1for and myo7b2rev; primer sequences TGCGCGC-AGAACCCCCCACCTGGC and GCCAGGTGGGGGGTTCTGCGC-GCA, respectively) and a polymorphism between C57BL/6J and *M. spretus* that was assayed by an *Msp*I digest of PCR products. A total of 188 DNA samples were typed.

A human genomic fragment of 3 kb was amplified using the human myosin-VIIb primers H-MY7bfor and H-MY7b11rev (GCTCAT-GGGGGTGAGTGCTGAGGA and ACTCAGGAGGCTGAGGTGG-GAGAA, respectively) and cloned. The genomic fragment was used for fluorescence *in situ* hybridization (FISH) mapping in human as previously described (Garcia-Anoveros *et al.*, 1997).

Northern analysis. A mouse multiple-tissue Northern blot from Clontech (BALB/c, 8–12 weeks) was hybridized with a myosin-VIIb-specific probe (clone 333893 from the IMAGE Consortium, Accession Nos. W15882 and AI391272). Labeling and hybridization were performed as described previously (Chen *et al.*, 1996).

In situ hybridization. Mouse embryo sections were hybridized with a 440-bp riboprobe prepared from a mouse myosin-VIIb cDNA fragment (4653–5093), using the protocol described in Strong *et al.* (1993).

Phylogenetic analysis. Phylogenetic relationships were determined by alignment of the predicted amino acid sequences using ClustalX (Thompson *et al.*, 1997). Sequences were obtained from GenBank, with accession numbers as noted. Trees were calculated by ClustalX with 2000 bootstrap trials, excluding positions with gaps and correcting for multiple substitutions, and were separately calculated using the PROTPARS program in PHYLIP [Felsenstein (1993), http://evolution.genetics.washington.edu/phylip.html]. Trees were displayed for plotting with TreeView 1.5 (http://taxonomy.zoology.gla.ac.uk/rod/rod.html).

Secondary structure predictions were made using the Protein Sequence Analysis Server at Boston University (http://bmerc-www.bu.edu/psa/), using single-domain discrete state-space models (White *et al.*, 1994).

Preparation of myosin-VIIb-specific antibodies. To create antibodies, a *Pst*I fragment from nt 2740 to 3780 that encodes the final two IQ motifs and the first MyTH4 domain was inserted into pGEX-2T (Pharmacia Biotech). The resulting plasmid was introduced into XL1-Blue bacteria (Stratagene) and, after induction with 0.3 mM IPTG, produced a glutathione *S*-transferase–myosin-VIIb-tail fusion protein (GST–M7B), which was insoluble. Therefore, the protein pellet after sequential 1% T × 100 and 0.1% Sarcosyl extraction was recovered in PBS + 0.1% SDS and used directly as the immunogen for injection into rabbits.

To affinity-purify the serum, a second fusion protein was created. A myosin-VIIb cDNA fragment (nt 1950–3595) was ligated into pQE-32 (Qiagen) to create a polyhistidine-tagged M7B-tail fusion protein (HIS–M7B). After purification on a nickel-Sepharose column (Qiagen), the concentrated HIS–M7B was dialyzed into carbonate buffer and coupled to cyanogen bromide-activated Sepharose (Pharmacia). Serum was diluted 1:1 with 50 mM Tris–HCl, 150 mM NaCl, pH 7.5 (TBS) before application to the affinity column. Specific antibodies were eluted at low pH and dialyzed into TBS + 0.02% sodium azide before use.

Immunoblot analysis. Proteins were isolated and separated on 5–20% polyacrylamide gels as described (Hasson *et al.*, 1995). Separated proteins were transferred to nitrocellulose, and the filter was blocked with 5% nonfat dry milk in TBS and incubated with 0.5 μg/ml anti-myosin-VIIb antibody in TBS + 0.05% Tween 20 for 2 h at room temperature. Filters were washed and incubated for 30 min with 40 mU/ml POD conjugated anti-rabbit IgG (Boehringer Mannheim) and then washed before detection using a chemiluminescence detection kit (ECL; Amersham).

Indirect immunofluorescence. Frozen sections of mouse kidney and intestine were prepared as described (Hasson and Mooseker, 1994). Slides were thawed and extracted in −20°C acetone for 5 min before use. Slides were stained essentially as described for whole mounts in Hasson *et al.* (1995), except that sections were incubated

[2] The HGMW-approved symbol for the gene described in this paper is MYO7B.

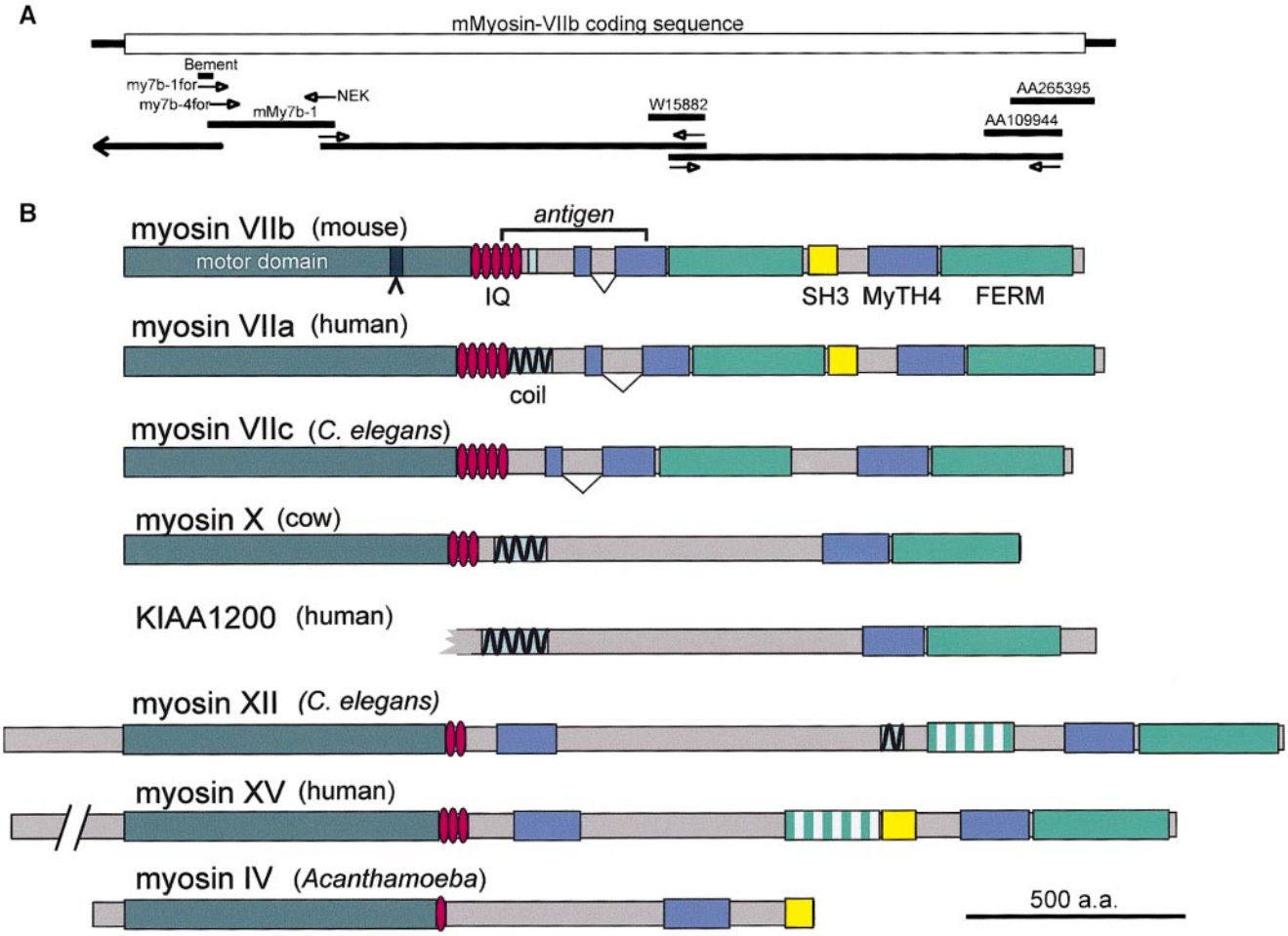

FIG. 1. Cloning strategy and domain structure of myosin-VIIb. (**A**) Primers used to amplify cDNA of mouse myosin-VIIb and clones assembled for the complete sequence. Clones are named as described in the text, and accession numbers represent ESTs that were obtained and sequenced. (**B**) Domain structure of myosin-VIIb and other proteins with MyTH4 domains. Indicated in each (if present) are the motor domain, the light-chain-binding IQ motifs, a predicted coiled-coil domain, the MyTH4 domains, the FERM domains, and the SH3 domain. Very divergent FERM domains are shown as striped green. The region of mouse myosin-VIIb used as an antigen is indicated. Domain boundaries for mouse myosin-VIIb are: head aa 1–760, IQs aa 761–887, MyTH4 aa 989–1189, FERM aa 1202–1499, SH3 aa 1502–1559, MyTH4 aa 1611–1790, FERM aa 1803–2099. Corresponding nucleotide boundaries are in Accession No. AF242411. Accession numbers are as follows: mouse myosin-VIIb, AF242411, human myosin-VIIa, U55208; *C. elegans* myosin-VII, U80848; cow myosin-X, U55042; human KIAA1200 AB033026; *C. elegans* myosin-XII, CAA91469; human myosin-XV, AF144094; *Acanthamoeba* myosin-IV, P47808.

overnight at 4°C with 5 μg/ml affinity-purified anti-myosin-VIIb antibody and then incubated for 1 h at 37°C with a 1:120 dilution of FITC-conjugated donkey anti-rabbit secondary antibody (Amersham) plus 80 nM rhodamine-conjugated phalloidin (Molecular Probes).

In other experiments, we used an antiserum to human platelet (nonmuscle) myosin (BT-561, Biomedical Technologies). Slides were incubated for 1 h at 22°C at 1:20 dilution and then incubated for 1 h at 22°C with 1:400 dilution FITC-conjugated donkey anti-rabbit secondary antibody (Amersham) plus 80 nM BODIPY-conjugated phalloidin (Molecular Probes).

Mouse enterocytes were dissociated according to Cartwright and Higgins (1999), resuspended in MEM, and dried onto silane-coated microscope slides. The cells were then fixed in 4% formaldehyde for 5 min and extracted in −20°C acetone for 5 min. They were air-dried, rehydrated in PBS, blocked with 5% BSA and 1% NGS in PBS with 25 mM EGTA, and then washed. Cells were labeled with 5 μg/ml of myosin-VIIb antibody for 45 min at 37°C, washed 3× in PBS with 0.5% BSA, and labeled for 45 min with 1:200 FITC-conjugated goat anti-rabbit and 1:40 BODIPY-labeled phalloidin. Samples were observed with a Bio-Rad MRC1024 or with a Bio-Rad MicroRadiance confocal microscope.

RESULTS

Cloning of Mouse Myosin-VIIb

A small fragment of the human myosin-VIIb head domain was first cloned from human leukocytes and an epithelial cell line (Bement *et al.*, 1994). We extended the mouse myosin-VIIb sequence using RT-PCR between primers specific for this fragment and degenerate primers for a conserved sequence in all myosins (NEKLQQ). We next found two mouse ESTs that are similar but not identical to mouse myosin-VIIa and further extended the mouse sequence by RT-PCR with primers from these ESTs. RACE was then used to extend the sequence in the 5′ direction (Fig. 1; see Materials and Methods).

The resulting sequence contained an open reading frame of 6339 nucleotides, encoding a 2113-amino-acid protein of 240,786 Da predicted molecular mass. This

TABLE 1

Inferred Exon Structure of Human Myosin-VIIb

	exon 1	AAGATGACGAGGGCAAGGTCAGTGTTCTGGGGTTTCCTCTGG
GGGGAGTCTGCACCCATTGTTCCAGGAACACTGGATCCG	exon 2	AGCAGCACAAGATCTATGTGAGTCTCCCCAGCCCTGTGTCCA
CACTGACCACCTGCTTCCTTCCCAGACATACACAGGCTC	exon 3	CAGTGCTGCATCATCAGGTGAGGCAGAGGGGTCAGGCACCAC
ATGTCCCTGCACACCCTTTTTGCAGCGGCGAGTCTGGGG	exon 4	CAACCCCATCCTGGAGGGTAAGCATCACTCTGGGACCCGCCCT
ATGGGCATCGCCCGCTTACCTTCAGCCTTTGGAAATGCC	exon 5	CCCGGGTCTGCCGGCAGGTGAGGCCTCCCCCTTCCCAGGTCGG
CTGGAATGCCCTCCCTCCCTCCCAGGCTCCCGAGGAGCG	exon 6	ACCACTACCTGACCATGGTGAGCTGCCCACCTGCCGCCTCCCA
TTCACTGAGGCACCCTGTCCCTCAGGGGAACTGCACTTC	exon 7	GAATGTGGGGTTCATGGGTAATGCCGGTTCTGCCCCAACTGCAC
TCAGCATTCCTGCTTCTCTCTCTAGCTTCGGTCTTCGAG	exon 8	TGATGAAGTTACTGGAGGTAGGGGTGCTGTGCCCACAGCTTCCA
ACGCAGCCCCCACCTGCCTCCCCAGGTGCAGCACCAGGA	exon 9	GGGACGCCTTTGTCAAGGTACAGAGCTGAGAGAGCAGGGCTTAC
TTCTCCCACCCCCGTGTCTCTCCAGGGCATCTATGGGCA	exon 10	AATTTCGAGAACAATAGGTATGAAGATCTCAGATCCCAGCCCCA
CTGGGCAGTGACCTTGCCTCCACAGCTTCGAGCAGCTCT	exon 11	AAAGCCGCTTCCCGCAGGTGTGTGTTCGGGCCTGCCGACCTTCTG
CCACAGGGTGTCTGGGTTCTTCCAGGGGACAGATCTCAC	exon 12	GTACTACCAAGCAGAAGGTGGGTGCAGCTCTCCTCTCATGTCCCT
CTGGGTGGGCCCTGTGTCTCCACAGGCTTCCTGGAGAAG	exon 13	GAAACCATCTCTTCAAGGTGGGCTCCCAGGCACCCTCCTGGGTCT
TTGTGCTCTGTGCTTCCATTCACAGTCTGCAGACTCAAA	exon 14	AGTACAAGAAGCCGCTGGTAATGACAGGAGGCTGGGGCACAGCAA
GTCAGCGCCCGGTGTCCGCCCACAGCTGTTCGACCGGGA	exon 15	ACGCCATGCGGATGCAGGTCAGCGCCCCTCGGGGACGGTCACCTC
CGATACCCCCGTTTGGTCTTGGCAGCTGCAAGGCAACGT	exon 16	CAAAAATTTTCCTGAGGGTGAGACCCCGAGGAACCAGCCAGCTGTC
AGTGACGGCGTCTCTCCTGTTCCAGGATCATCAGGACAC	exon 17	CGGGGCTACAGATACAGGTGCCGGCCCCACCCCAAGGCCCACCCAG
TGTGTGGCTTGCATTGCCCTTCTAGGAAGGATGTCCTGA	exon 18	GTAGGAATTTCAAGCTGGTGAGAGAGCTCTCTGGGGCGGCTGGGCC
TCTCACCTCTCTCTTGCCTCCGCAGATCCTCGTGGGCTT	exon 19	AGCAAAGGAAGGCCAATGTAGGTGGTCACCTGGCCTCTTGGGCAGG
TAACCTTCCTCCACGGGGTATGCAGGCGCCGCTGGTCAT	exon 20	CCTCGCCGCACTTTGAGGTAACACAAGCCTGGTGTCCACAATCCGC
CCGTGTTCTCCCTCAATGGCCGTAGGATCTGGAATCGAA	exon 21	ATGACACTGACTGCTTGGTACCAGGGTTCACTGGCTTCTAGTGGAT
TGGGCCTTCTGTCTTGTTTCCCCAGGCCGCCCTGGTCAT	exon 22	ACAGTAGATCTGCACAGGCAAGTGGGGGGCAGCAGCGGGCAGAGGA
CTGATGGCTGCCTTTGGGTTTCAAGGTGGCCAGCCAGCT	exon 23	CTGCGGCCCAGCCTCAGGTCAGTTCCCACTCCCATCCCGGCCCCAT
TCTCCTAATGGTCTGTGTCTTTCAGGGATGAGATTTACT	exon 24	CAGAGAGGTTCATGAAGGTGAGAGGGTTCATGAAGGGAGGGCGGGC
CCCTTCTCCCCTCCTCACCCACCAGTATCTACTGAACTT	exon 25	CCTGGCTGGAGCTGCAGGTAGGGGCTGGCAGGGGTGAGAGCGGGCA
GGAACTGAATCTCATCTGTCCCCAGGCTGTCAAGTCCAA	exon 26	TCGCCGTGTACGACAAGGTACCAGCCAGGCACCCTGCCCGTCAGCC
CCCTGCTCCCCGACTCTGGCCTCAGTTCTGGTCCCTGGG	exon 27	AGTACAGCTTCGAGAAGGTGAGGGGCCTGAGAGCCAGGTCCACCCT
CCCGTGGGTGCCCTGGGCTGTGCAGGAGGAAGAGCTGGT	exon 28	CTGCCGCCTGCGCCAAGGTCAGCCTGCATGCAGCTCAGGCACCCAC
GGTGACATCCAGGATCCCCCCTCAGGCCCCATACACTCA	exon 29	AGTCATCACACTCTCAGGTAATGGCATCTGACAGGGGGCAGGGAGC
TCACACTGCCGTCTCTCCTGGCCAGGCCCCCGCCTGCCC	exon 30	GGTCTGGCCACCAACAGGTGCGGGCCCTGAGGGAAGATCTCTTCTT
TGGTCACGCTGTCCTTCATCTCCAGGGAGGCCCAGGGCG	exon 31	GGACAGGAAGGCCACAGGTGCCAGACTGGGTGGGGTGGGGTGGGGT
GCAAATAGCCTCCCTGCCCTTACAGATGACACCACCCTC	exon 32	CCTCGGCACAGCTGCTGGTAACTGGCACGCTCCCCTGTCCTCAGCC
ACCCACAGGCCTGTGCCCCCTTCAGAGCTTGCTTGCCAT	exon 33	TCCTATGAGTTCTTCAGGTGCCCCCCAGCCCCGCTCCGCCTCATTG
TCACACCAGCCTCTAACCTCACAGGGGCTCCAGAGAAGG	exon 34	TCGCCTGCCAGATCTTTGTCGATATCCTTCCCCACCAGCCTGCCTG
GCCCCAGCACTGTGCTCCTTGACAGCCACACCCATCCTC	exon 35	ACGCACAACTCCAACAGGTCTGCTGGGGCGGCGGCCAGCCCACGCG
CCGGCTGACAAGTGCTACCCTTCAGGCACAGCGAAGAGC	exon 36	ATCCAGAAGGTCCTGAGGTGAGCCCAGTGCCTCCAGCCCCCAGCAT
CTGCAGCACACGCTGTCCCCCTCAGGACGGGGCCCCGGA	exon 37	CCAATGACACCAGTGAGGTGAGGCCCTGCTCTGGTCTGCACGGCAA
CCTCACCAGCTGCCTCTCTGTCCAGATGCTGGAGGTGGT	exon 38	TCAAGATTTCAGACAAGGTGGGCCGGGCTGGGGCTGGGCAGACGGT
TTCCCTGTACCTTCCCCTTCCCCAGGTCATCAGCCAGAA	exon 39	CAAGCCCCAGAAAGAAGGTGAGGAGGCCTCTGTGGAGCTGGGGGAG
GTGCCCACTGCTGGCCCTCGCCCAGGGGCCCCCGTGACG	exon 40	TACTCCATTACCACCAGGTACCGGGCAGGCTGCCCTGGTGGGCACT
CATGCCCAGTGTGTCCATCACCCAGGAGCTGCCCAAGTA	exon 41	CGGAGGAGTGGAAAAAGGTCCCTGGTCGGGCTGGGGAAGGGTTCTT
CCTTACTGGCCCTCCTGTCCCCCAGAGCATCCTTCTAGC	exon 42	CCTTCTTCGAGGTGAAGGTAAACCTTGCCCCACGCCAGGGCCTCCT
TGACCGCCGTGTCCCTCCCTCCCAGCAAACCTCGGAGCC	exon 43	TCCACCCCAAGACCAAGGTAGCTGCTGGGCCTCCGGAGGGGCTGGG
GCCCACCCACCCTCTCTGCCCCCAGGACCTGCTCACCAC	exon 44	TGTGCGAGACCTCCCTGGTGAGCTCAGGTTCTTTCTCCCATCCAAG
TCTGACCCCCCCGTCCCCTGTCCAGGGCTATAAGATGGA	exon 45	TGACCTGCTGACCTCATATGTGCAGCAGCTCCTGAGTGCCAT
GAACAAGCAGCGGGGCTCCAAGGCCCCAGCCCTGGCCAGCACCTAGCAGCGGATGCTGGCGTGTCTGCTCAGGCGCCCTTCCCGACCTCTAGC		
CTGGCGGCACCTTCCCAGGCCCTCTCAACCCAGGGCCTGTCCTTGGCGGGCAGCCTTCCATGCTGCCCCCCATACAAAGCCCACTCAGCCCCG		
CAGGCGGCCCCCTCTGTCCTGGGCGCTGCCCAGGGAGGCCAAAAGACGGGCCCAGAATGGGGTCGGGAGTCTCGGACCCCCAGGCTATTGGTG		
GATGACTGACTGACAGGACACCTCCCAACCCCACCCCACCCCACCAGAATGTTC**AATAAA**AACTCCTGGAGCAGGAGAAGTGTGTCTGTCTGA		
GGGA		

Note. Sequence was derived from a human BAC (Accession No. AC010976), and splice junctions were deduced by comparison to the mouse cDNA and by searching for consensus splice sites. Exon–intron boundaries are shown, with exonic sequence underlined and in a larger font. The polyadenylation signal, AATAAA, is indicated in boldface type.

protein is 54% identical overall to myosin-VIIa (Accession No. U55208; Chen *et al.*, 1996) and 44% identical overall to a *Caenorhabditis elegans* myosin-VII (HUM-6; U80848). In the conserved head domain, it is 62% identical to human or mouse myosin-VIIa, 50–54% identical to other myosin-VII isoforms from *C. elegans* and *Drosophila melanogaster*, but only ~40% identical to myosins of all other branches. Similarly, a phylogeny analysis based on the head domains of 43 myosins, representing 15 classes, showed that this protein is much more closely related to type VII myosins than to any other class (data not shown), confirming its original designation as myosin-VIIb.

Sequence and Exon Structure of Human Myosin-VIIb

We first used the predicted amino acid sequence to search for human ESTs representing myosin-VIIb. Ten such ESTs, included in the *Homo sapiens* UniGene cluster Hs.154578, represent the last 123 amino acids and the 3′ UTR of human myosin-VIIb. We then searched the High Throughput Genomic Sequence database in GenBank for human genomic sequence that would correspond to myosin-VIIb and found two such entries. A complete exon structure was deduced by comparison of the mouse myosin-VIIb sequence with two human BACs (Accession Nos. AC010976 and

AC010898). The human gene contains 45 exons (Table 1). The predicted amino acid sequence is 88% identical to the mouse myosin-VIIb sequence, a much higher identity than with any other myosin, indicating that this gene represents human myosin-VIIb.

Chromosomal Mapping

Using the original 130-bp human fragment (Bement *et al.*, 1994) as a probe, we had previously mapped the mouse myosin-VIIb gene to chromosome 18, near *Apc* (Hasson *et al.*, 1996). However, this human probe also detected a different *Hin*dIII fragment that mapped to mouse chromosome 11 near *Zpf*. To determine which map position is correct, we used The Jackson Laboratory Backcross Panel to map mouse myosin-VIIb. The allele pattern of myosin-VIIb was compared to the 3900 other loci previously mapped in the backcross panel. The gene mapped 0.5 ± 0.5 cM proximal to D18Mit12, approximately 14 cM from the centromere of chromosome 18 (Fig. 2). Because the backcross-panel mapping used specific PCR primers based on the mouse sequence, whereas the previous mouse mapping used a short human probe, this confirms the original assignment to chromosome 18 near *Apc*. The alternative localization to chromosome 11 using the human fragment may have detected partial homology to another related gene or a pseudogene. There are no mutant mouse mutant loci in the region of D18Mit12 for which myosin-VIIb is a reasonable candidate.

Radiation hybrid mapping information of STS marker A006H45 on the human BAC was used to localize human myosin-VIIb to 137 Mb on chromosome 2, corresponding to the cytogenetic location 2q21.1. We confirmed this localization using FISH with a 3-kb genomic probe derived from the human clone hMy7b-1, which contains two myosin-VIIb exons (data not shown). There are no human disease loci in this region for which myosin-VIIb is a reasonable candidate.

Predicted regions of homologous synteny between mouse and human indicate that mouse chromosomal locus 18.0–8 corresponds to human chromosome 18 and that mouse 18.11–29 corresponds to human chromosome 5. However, two genes located near myosin-VIIb at mouse 18.14–15 map to human chromosome 2 (Mao *et al.*, 1999; see also NCBI Human–Mouse Homology Map, http://www.ncbi.nlm.nih.gov/Homology/mouse18.html). Our data indicate that human myosin-VIIb is also located on chromosome 2, which confirms the additional syntenic relationship whereby mouse 18.14–15 corresponds to human chromosome 2.

Domain Structure

Myosin-VIIb has an overall organization very similar to that of myosin-VIIa (Fig. 1B). Compared to other type VII myosins, the conserved head domain has an insert of 19 aa, at a location (aa 600–618) that corresponds to the "50–20" junction in the myosin head structure. This region forms a variable loop in other

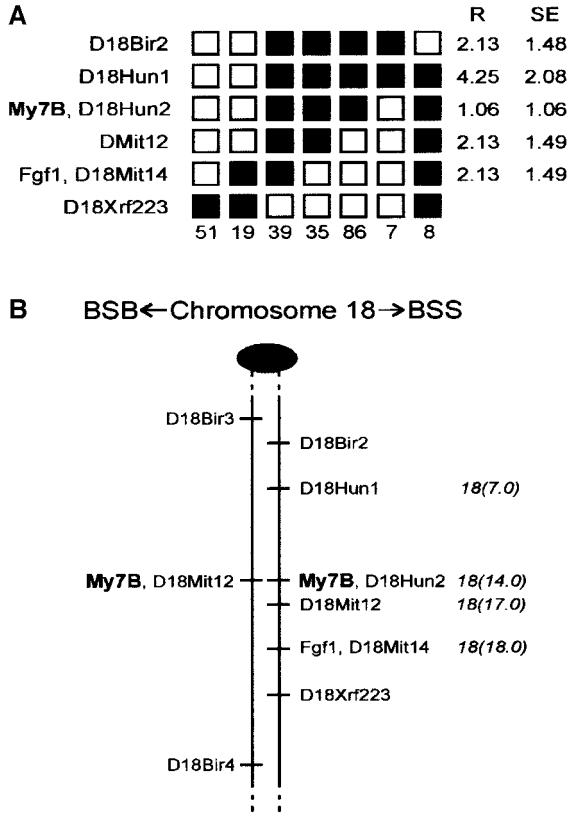

FIG. 2. Backcross mapping of mouse myosin-VIIb. (**A**) Haplotype figure from The Jackson Laboratory BSS backcross showing part of chromosome 18 with loci linked to myosin-VIIb. Loci are listed in order with the most proximal at the top. The black boxes represent the C57BL6/JEi allele, and the white boxes represent the SPRET/Ei allele. The number of animals with each haplotype is given at the bottom of each column of boxes. The percentage recombination (R) between adjacent loci is given to the right of the figure, with the standard error (SE) for each R. Missing typings were inferred from surrounding data where assignment was unambiguous. (**B**) Placement of the myosin-VIIb gene (myo7b) relative to other markers on mouse chromosome 18.

members of the myosin superfamily (Cope *et al.*, 1996). Like myosin-VIIa, myosin-VIIb has five IQ domains (aa 761–877) thought to bind regulatory light chains such as calmodulin. Myosin-VIIb is missing the coiled-coil domain that follows the IQ domains of myosin-VIIa.

The tail of myosin-VIIb contains a repeated domain of about 500 aa. Each repeat has a MyTH4 domain of about 150 aa (aa 989–1189 with a gap at 1028–1084, and aa 1641–1790), similar to domains in myosins of classes IV, VII, X, XII, and XV and in a plant kinesin (Chen *et al.*, 1996; Liang *et al.*, 1999; Berg *et al.*, 2000). All known MyTH4 domains are aligned in Fig. 3, along with a secondary structure prediction based on the consensus sequence. This domain appears largely alpha-helical, interrupted by three or four turns. Certain missense mutations in the MyTH4 domains of mouse myosin-VIIa, human myosin-VIIa, and human myosin-XV cause deafness; these are circled in Fig. 3. Four highly conserved regions of the MyTH4 domain are indicated in Fig. 3 as MGD (consensus sequence $L^{K}/_{R}{}^{F}/_{Y}$ MGDhP), LRDE (consensus LRDEhYCQhhKQhxxN),

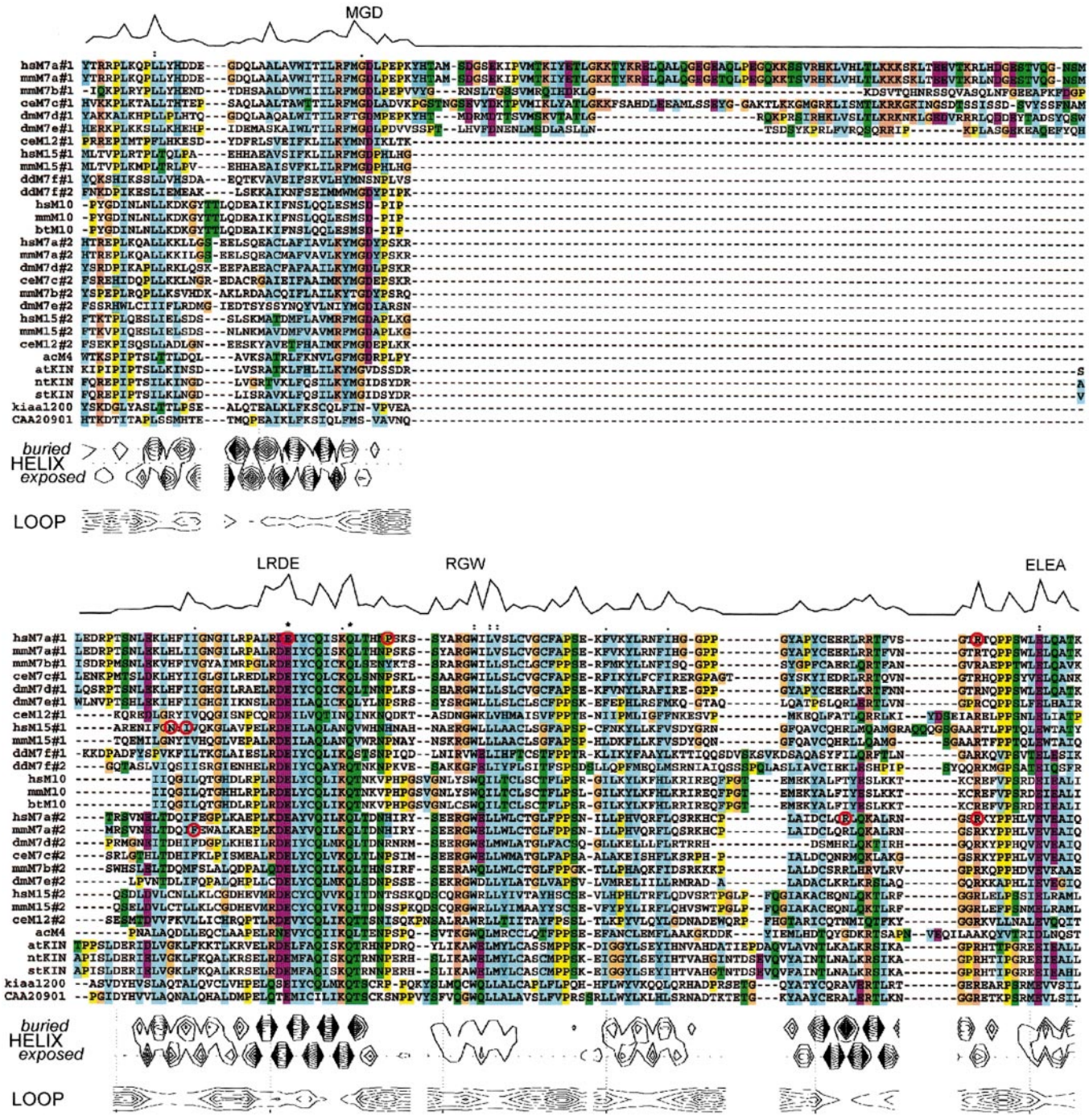

FIG. 3. Alignment and predicted secondary structure of all known MyTH4 domains. Domains are denoted by species (e.g., hs), superfamily (M-myosin, KIN-kinesin), family (e.g., 7a), and order when more than one MyTH4 domain occurs in a protein (e.g., #2). Residues are shown on a colored background when they occur in a conserved position with identical or similar residues (orange, Q; yellow, P; green, TSNQ; blue, WLVIMAFC; pink, C; cyan, HY; magenta, DE; red, KR). Above the alignment is an indication of the degree of conservation at each residue position. Below the alignment is secondary structure predicted for the consensus, for helix and loop configurations, by the Protein Sequence Analysis Server at Boston University. Strand predictions are not shown but were generally of low probability. Strength of prediction is indicated as a probability topography, so that a larger number of lines indicates higher probability. Residues circled in red are mutated in various inherited deafnesses. Species are abbreviated as follows: hs, *Homo sapiens;* mm, *Mus musculus;* bt, *Bos taurus;* ce, *Caenorhabditis elegans;* dm, *Drosophila melanogaster;* dd, *Dictyostelium discoideum;* ac, *Acanthamoeba castellanii;* at, *Arabidopsis thaliana;* nt, *Nicotania tabaccum;* st, *Solana tuberculosum*. Homologues of myosin-VII are listed as a, b, c, etc., for the purposes of this figure. Accession numbers are as follows: hsM7a, U55208; mmM7a, U81453; hsM7b, AC010976; mmM7b, AF242411; ceM7c(HUM6), U80848; dmM7d(35B), AAF44915; dmM7e(28B), AAF52536; ddM7f, AAF06035; btM10, U55042; mmM10, CAB56466; hsM10, AF247457; ceM12(HUM4), CAA91469; acM4(MyoI), P47808; hsM15, AF144094; mmM15, AF144095; stKIN, L46702; ntKIN, U52078; atKIN, AF002678; KIAA1200, AB033026.

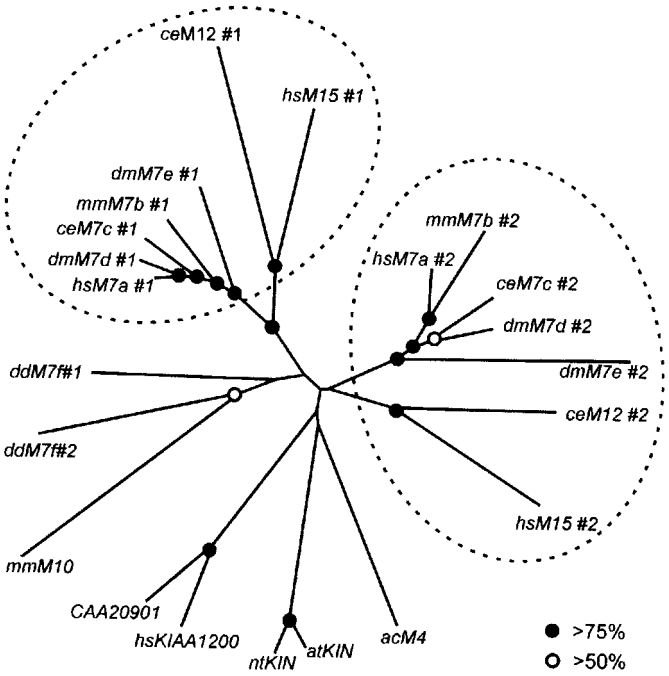

FIG. 4. Phylogeny of MyTH4 domains. The alignment shown in Fig. 3 was used with ClustalX to calculate an unrooted phylogeny tree for the individual MyTH4 domains, excluding positions with gaps and correcting for multiple substitutions. In myosins that have two MyTH4 domains, the first of each (#1) and the second of each (#2) are circled on the phylogeny tree, with the exception of *Dictyostelium* myosin-VII. When there was virtually no separation between orthologues, such as hsM7a and mmM7a, one was removed for clarity. Filled circles indicate nodes at which branches were joined in >75% of 2000 bootstrap trials, and open circles indicate >50% joining. Similar results were produced from calculations without correction for multiple substitutions or without excluding gaps or from the parsimony method of the PROTPARS program of PHYLIP. Species are as in Fig. 3.

RGW (consensus RGWxLh), and ELEA (consensus RxxPPSxhELEA), where h indicates a hydrophobic residue and x is any residue. Of these, the LRDE sequence is the most highly conserved. It is strongly predicted to form an amphipathic helix, with the three absolutely conserved residues (E-Q-Q) forming a polar stripe along one side. Two of the deafness-causing mutations in myosin-VIIa fall in the RDE segment. The initial arginine of the ELEA segment is also almost perfectly conserved, and point mutations of that arginine in either the first or the second MyTH4 domain of myosin-VIIa cause Usher syndrome 1B. Altogether, eight known disease-causing mutations occur in the MyTH4 domains of myosins.

Phylogenetic studies of myosin based on the head domain have shown early divergence of 17 different classes (Cheney *et al.*, 1993; Hodge and Cope, 2000). These conserved regions of the tail offer a basis for additional phylogenetic analysis. Whereas myosins of classes IV and X have a single MyTH4 domain, myosins of classes VII, XII, and XV have two MyTH4 domains, perhaps arising from a duplication of the tail portion of an early ancestral gene. A phylogeny of the MyTH4 domains in Fig. 3, created with the neighbor-joining algorithm of ClustalX (Fig. 4), indicates that the first MyTH4 domains of these three classes are more closely related to one another than to the second MyTH4 domains. Thus the duplication most likely occurred before the separation of myosin classes VII, XII, and XV. In addition, neither predicted MyTH4 domain of *Dictyostelium* myosin-VII (Accession No. AAF06035) is as closely related to other myosins-VII or to myosins-XII and -XV. This and other phylogenic analyses (Titus, 1999; Hodge and Cope, 2000) indicate that it is the most divergent branch of that class, perhaps forming a separate class.

The phylogentic analysis was then repeated using the FERM domains, with quantitatively similar results: myosins-VII, -XII, and -XV segregate together; among these three classes the second FERM domains segregate separately from the first, and *Dictyostelium* myosin-VII is most divergent.

In each repeat, the MyTH4 domain is followed by a domain (aa 1202–1499 and aa 1803–2100) with similarity to talin, ezrin, radixin, and moesin. Referred to as a talin-homology domain in our description of myo-

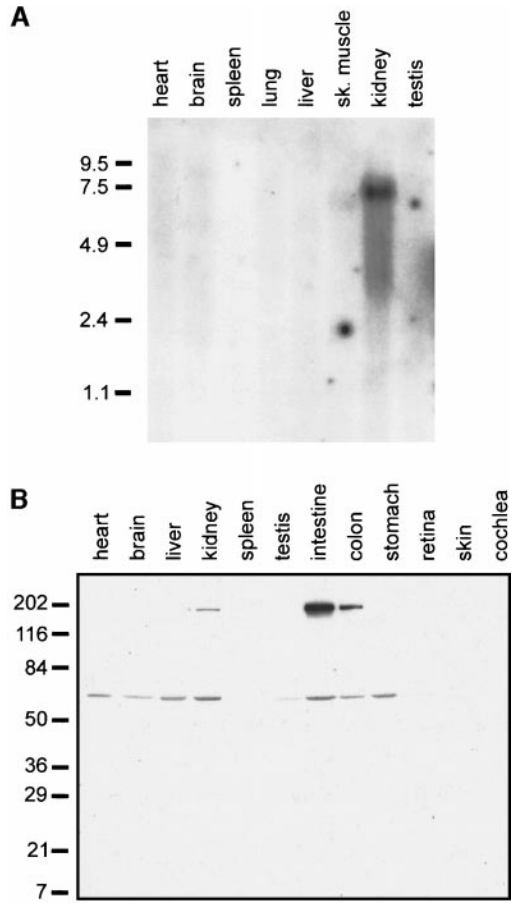

FIG. 5. Expression of myosin-VIIb in different tissues by Northern blot and immunoblot. (**A**) A multiple-tissue Northern blot shows a single band of about 7.5 kb in kidney, and no significant presence in the other tissues shown. (**B**) An immunoblot, using an antibody directed against the tail region of myosin-VIIb (indicated in Fig. 1), shows the strongest expression in the intestine, with additional expression in colon and kidney. The upper band, running near 200 kDa, is myosin-VIIb.

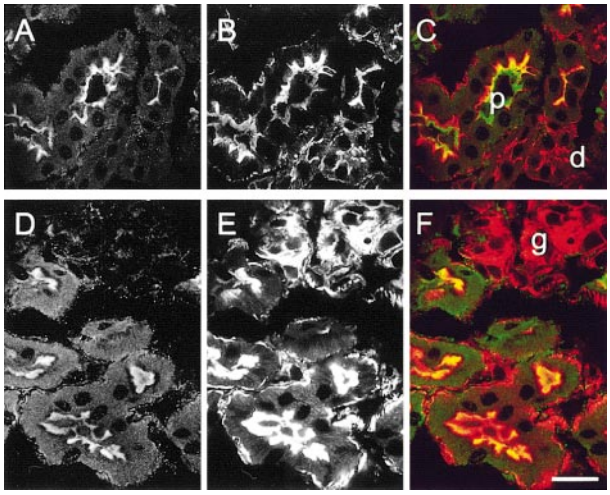

FIG. 6. Localization of myosin-VIIb in kidney by immunohistochemistry. The myosin-VIIb label is shown in green, the actin label is shown in red, and colocalization is shown in yellow. Myosin-VIIb is expressed by proximal tubule cells (p) in mouse kidney where it is present in the apical microvilli. It is not expressed in distal tubules (d), in glomeruli (g), or in blood vessels (not shown). (**A, D**) Myosin-VIIb; (**B, E**) F-actin; (**C, F**) overlay. Scale bar indicates 25 μm.

sin-VIIa (Chen *et al.*, 1996), this is now termed a FERM domain (Chishti *et al.*, 1998). In other proteins, FERM domains bind to cell-surface transmembrane proteins, linking these proteins to the actin cytoskeleton (Chishti *et al.*, 1998).

Following the first FERM domain, myosin-VIIb has a predicted SH3 domain (aa 1502–1559) that contains most of the canonical residues of other SH3 domains. Several other myosins with MyTH4 and FERM domains also contain SH3 domains in a similar position (Mburu *et al.*, 1997; Liang *et al.*, 1999). SH3 domains also occur in certain members of the myosin-I class, such as *Dictyostelium* MyoA and MyoB, yeast Myo3, and human myosin-Ic (Coluccio, 1997). SH3 domains mediate protein–protein interaction, by binding to proline-rich motifs such as PxxP (Kuriyan and Cowburn, 1997). There is a suggestion that the SH3 domain in myosin-XV might mediate intramolecular binding to the proline-rich segment preceding the first FERM domain in myosin-XV (Liang *et al.*, 1999). This may be true only for myosin-XV, since there is not a similar proline-rich domain in myosin-VIIb or other myosins of this general architecture.

Expression of Myosin-VIIb

To gain insight into the function of myosin-VIIb, we identified which tissues express the gene and where the protein is located within cells. In a Northern blot, using the clone from EST W15882 as a probe, a myosin-VIIb message of about 7.2 kb was observed in kidney and not in other tissues included on this blot (Fig. 5A). A probe for *in situ* hybridization was constructed from a cDNA fragment (nt 4653–5093) and used to determine the expression pattern in embryonic mice. At embryonic day 17, strong label was seen in the enterocytes of the intestine (data not shown), but not other tissues.

We then made a rabbit antibody to the tail of mouse myosin-VIIb, specifically to the tail region shown in Fig. 1. On immunoblots containing protein from 12 different mouse tissues, the antibody recognized a band of approximately the predicted molecular weight in intestine, colon, and kidney, with the strongest expression in small intestine (Fig. 5B). The immunoblot thus confirms the expression in kidney found by Northern blot, but indicates much stronger expression in intestinal tissues (which were not included in the Northern blot). A smaller band of about 70 kDa was recognized in some tissues, suggesting cross-reactivity with another protein. However, only those tissues showing immunoreactivity to a high-molecular-weight band in blots could be labeled with the antibody in sections, so that cross-reactivity was limited to immunoblots. We did not detect expression in either retina or cochlea, despite the initial PCR of a fragment of myosin-VIIb from cochlea. If present in those tissues, myosin-VIIb may be expressed by only a small subset of cells.

In sections of mouse kidney (Fig. 6), the myosin-VIIb antibody revealed nearly exclusive localization of myosin-VIIb in the apical microvilli of cells lining the proximal tubules. There was also fainter labeling of the cell bodies of these cells. Myosin-VIIb was not seen in distal tubules or in the glomeruli.

In small intestine, the antibody lightly labeled the cell bodies and strongly labeled the apical surfaces of fully differentiated enterocytes (Fig. 7A). It did not label the goblet cells or the crypts. Label was specifically associated with the brush border, as revealed by phalloidin label of the brush border actin, and appeared to be most intense in the distal part of the microvilli (Figs. 7B–7D). To verify that we could distinguish actin staining in the terminal web versus microvillus, tissue sections were also stained with antibodies to myosin-IIa, which previous studies have shown is restricted to the terminal web region. As observed in other species, myosin-II colocalizes with actin only at the basal, presumed core rootlet portion of the actin within the brush border (Figs. 7E and 7F). In many of these images (Figs. 7A, 7D, and 7E), the (green) myosin-VIIb label appeared to occur beyond the most distal extent of the (red) microvillar actin. However, this may result simply from the much greater intensity of the green signal. Indeed, higher-resolution images of isolated enterocytes show the myosin-VIIb label to be coincident with the most distal actin label (Figs. 7G–7I). The localization profile of myosin-VIIb is thus unlike that of other known myosins associated with the brush border cytoskeleton, which include brush border myosin-I, myosin-Ic, myosin-IIa, myosin-V, and myosin-VI (Heintzelman *et al.*, 1994; Skowron *et al.*, 1998).

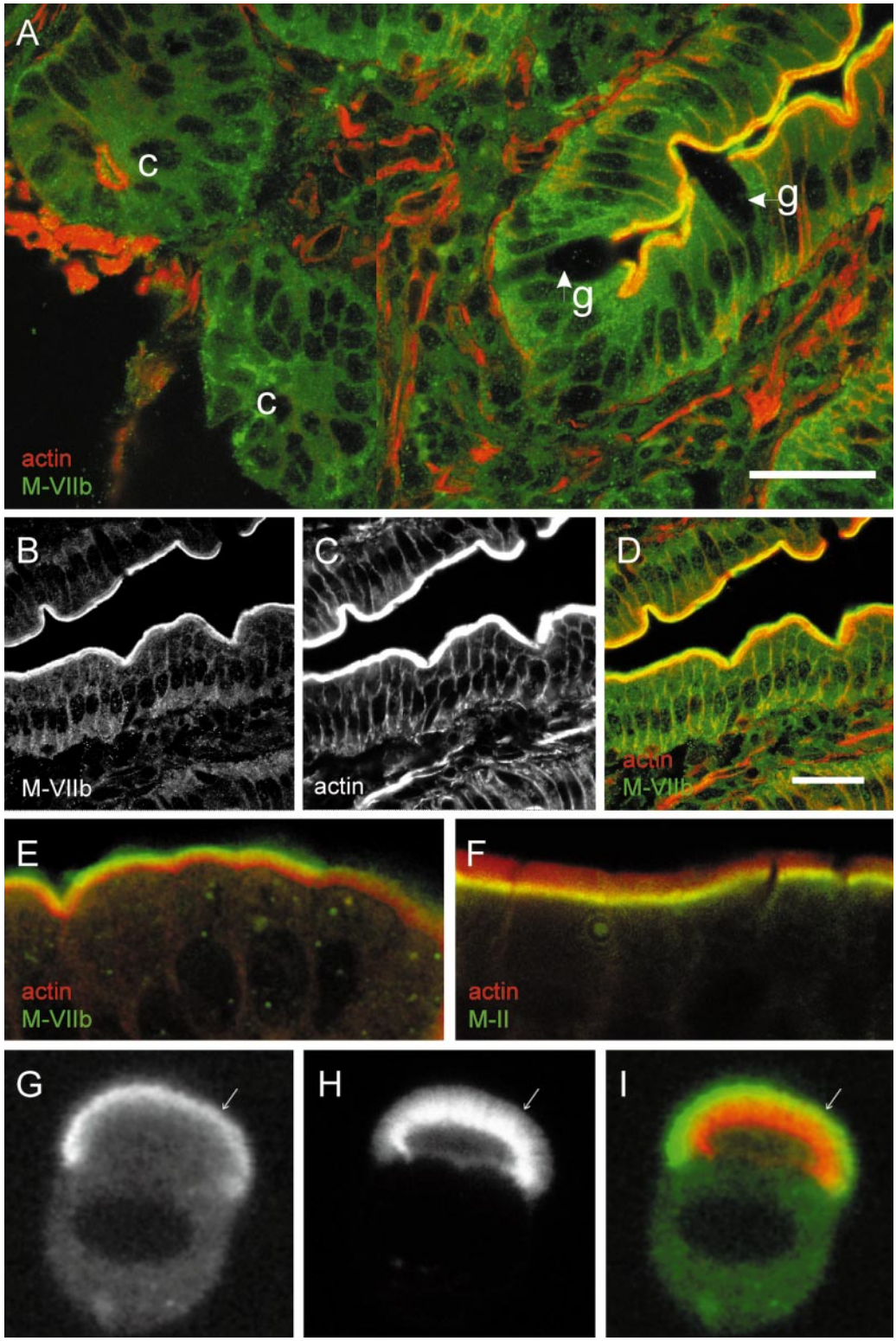

FIG. 7. Localization of myosin-VIIb in intestine by immunohistochemistry. In frozen sections of intestine, actin was labeled with phalloidin and is shown in red; myosin-VIIb or myosin-II was labeled with antibodies and are shown in green. (**A**) Myosin-VIIb is expressed by the enterocytes in mouse intestine, where it is concentrated in the apical brush border. It is not expressed by goblet cells (g, arrows). In the intestinal crypts (c), even those with apical actin assembled, myosin-VIIb does not localize to the apical domain; rather, it appears only in the apical brush border in the fully differentiated enterocyte. (**B–D**) Myosin-VIIb is especially concentrated at the distal tips of microvilli in enterocytes, as shown by the green label overlapping the most lumenal part of the red actin label. (**B,** myosin-VIIb; **C,** F-actin; **D,** overlay). (**E–F**) The distal localization of myosin-VIIb in microvilli (**E**) contrasts with the localization of myosin-II in the terminal web (**F**). (**G–I**) A similar distribution of myosin-VIIb can be seen in dissociated enterocytes. Myosin-VIIb label is found throughout the cytoplasm of enterocytes but concentrated in the tips of microvilli. The most distal myosin label (G) is at the same point as the most distal actin label (**H,** arrow). Scale bar indicates 25 μm (**A–D**).

DISCUSSION

The protein represented by the sequence assembled from mouse cDNA and from human genomic DNA is clearly of the myosin superfamily, based on the strong similarity of the head domain to other myosins (~40% identity). The domain structure of the tail and a phylogenetic analysis based on the head sequence both place it within the myosin-VII branch (50–60% identity). Within that branch, it is nearly equally divergent from mammalian myosin-VIIa, from *C. elegans* myosin-VII, and from two other *Drosophila* myosins-VII.

Myosin-VIIb is very similar to myosin-VIIa but differs in the absence of a predicted coiled-coil domain, which may indicate that myosin-VIIb functions as a single-headed motor, whereas myosin-VIIa is double-headed. It also differs in having a short insert in the head, near the 50–20 junction, termed loop 2. Variability in this loop in myosins-II directly affects binding to actin and, in turn, affects velocity (Knetsch *et al.*, 1999). Therefore, myosins-VIIa and -VIIb may also move on actin at different rates.

Along with the recently cloned myosin-XV (Liang *et al.*, 1999), myosin-VIIb expands the number of myosins that have a similar tail architecture. Five of the 17 known myosin classes contain both MyTH4 domains and FERM domains, sometimes in multiple representations, and 3 of these contain SH3 domains as well. The similarity among the tails of these distinct classes contrasts with an earlier view of myosins, in which the heads were conserved, but the tails were highly divergent and were thought to bind different kinds of cargo proteins. Myosins containing a MyTH4/FERM motif may still bind different proteins, but these are more likely to be of the same type and subserve the same general function. It will be very interesting to identify a binding protein in any one of the classes, as it may help elucidate the function of all such myosins. In the case of the plant kinesins, the MyTH4 domain may bind microtubules: Narasimhulu and Reddy (1998) found that a 250-amino-acid segment at the amino-terminus that includes the MyTH4 domain bound microtubules in an ATP-independent manner (discussed in Oliver *et al.*, 1999). As myosin-VIIa has been found in microtubule-containing structures such as the connecting cilium of vertebrate photoreceptors and the kinocilia of hair cells, the possibility arises that MyTH4 domains in myosins may couple actin filaments and microtubules in certain cytoplasmic regions.

The MyTH4 domain is paired with a FERM domain in all of these myosins but myosin-IV. Indeed, the phylogenetic distribution of the two domains is nearly identical: they are not in Archea or Bacteria, but appear in certain branches of the Eukaryota. Thus far, they are found in primitive eukaryotes such as *Dictyostelium*, but not in fungi; they appear in plants but only in a single plant kinesin whose orthologues have been noted in three species, and they are most widely found in Metazoa. It is tempting to speculate that the two domains were linked as a 500-amino-acid domain in some primordial eukaryotic protein that found its way only into certain branches of the eukaryotes. In some proteins, the MyTH4 portion may have been lost, leaving the FERM domain. In other proteins, such as myosins-XII and -XV, the FERM portion may have been lost or become nearly unrecognizable, leaving MyTH4 by itself.

A definitive function is not known for any of the myosin-VII family members. A *Dictyostelium* myosin-VII is essential for phagocytosis, but not for endocytosis in that amoeba (Titus, 1999; Hasson, 1999). However, that myosin is a very distant member of the myosin-VII group, and its function may not be closely related to that of myosin-VIIb. A much closer homologue is myosin-VIIa, expressed in the testis, retina, and inner ear of vertebrates. This myosin appears in the apical domain of epithelial cells, often associated with cilia and microvilli. For instance, myosin-VIIa in the sensory hair cells of the inner ear occurs in the stereocilia (microvilli) where it appears between the actin core and the membrane, and it appears to be associated with vesicles near the apical surface (Hasson *et al.*, 1997). Hair cells lacking myosin-VIIa fail to internalize aminoglycosides, suggesting a role in endocytosis or membrane recycling (Richardson *et al.*, 1997; Hasson, 1999). In photoreceptors, myosin-VIIa appears in the ciliary neck between inner and outer segments and appears to be important for transport of rhodopsin to the outer segment (Liu *et al.*, 1999). In cells of the retinal pigmented epithelium, myosin-VIIa is in the microvilli and may be involved in phagocytosis of photoreceptor outer segments (Hasson, 1999). In all these cases, then, myosin-VIIa is associated with membranes, especially of microvilli, and so may be involved in the shuttling of membrane-associated proteins.

Localization of myosin-VIIb within the microvilli of brush border epithelial cells of the proximal tubule and intestine fits this general pattern. These two epithelia are very active in transport of salts and nutrients, mediated by a variety of integral membrane pumps and channels. It seems possible that myosin-VIIb is involved in bringing these proteins to the microvilli or positioning them appropriately within microvilli. Alternatively, myosin-VIIb could play a role in regulating the transport activity of one or more of these microvillar membrane proteins, as has been proposed for the major microvillus-associated myosin of the intestinal brush border, brush border myosin-I (Wasserman and Fullmer, 1995; Mooseker *et al.*, 1991).

ACKNOWLEDGMENTS

We thank Drs. Ljiljana Jelaska and Gwenaëlle S. G. Géléoc for assisting with the experiments of Fig. 7, and Dr. LaDeana Hillier (Genome Sequencing Center, Washington University School of Medicine) for pointing out the STS marker in the human BAC containing myosin-VIIb. We appreciate comments on the manuscript from Dr. Heidi Rehm. This work was supported by a grant from the Deafness

Research Foundation (to T.H.), and by NIH Grants RO1-DC02281 (to DPC), R37-DK25387 (to M.S.M.), and P01-DK38979 (to Jon Morrow, Yale University). D.P.C. is an Investigator of the Howard Hughes Medical Institute.

REFERENCES

Avraham, K. B., Hasson, T., Steel, K. P., Kingsley, D. M., Russell, L. B., Mooseker, M. S., Copeland, N. G., and Jenkins, N. A. (1995). The mouse *Snell's waltzer* deafness gene encodes an unconventional myosin required for structural integrity of inner ear hair cells. *Nat. Genet.* **11:** 369–375.

Bement, W. M., Hasson, T., Wirth, J. A., Cheney, R. E., and Mooseker, M. S. (1994). Identification and overlapping expression of multiple unconventional myosin genes in vertebrate cell types. *Proc. Natl. Acad. Sci. USA* **91:** 6549–6553.

Berg, J. S., Derfler, B. H., Pennisi, C. M., Corey, D. P., and Cheney, R. E. (2000). Myosin X, a novel myosin with pleckstrin homology domains, associates with regions of dynamic actin. *J. Cell. Sci.* **113:** 3439–3451.

Cartwright, I. J., and Higgins, J. A. (1999). Isolated rabbit enterocytes as a model cell system for investigations of chylomicron assembly and secretion. *J. Lipid Res.* **40:** 1357–1365.

Chen, Z.-Y., Hasson, T., Kelley, P. M., Schwender, B. J., Schwartz, M. F., Ramakrishnan, M., Kimberling, W. J., Mooseker, M. S., and Corey, D. P. (1996). Molecular cloning and domain structure of human myosin-VIIa, the gene product defective in Usher syndrome 1B. *Genomics* **36:** 440–448.

Cheney, R. E., Riley, M. A., and Mooseker, M. S. (1993). Phylogenetic analysis of the myosin superfamily. *Cell Motil. Cytoskeleton* **24:** 215–223.

Chishti, A. H., Kim, A. C., Marfatia, S. M., Lutchman, M., Hanspal, M., Jindal, H., Liu, S.-C., Low, P. S., Rouleau, G. A., Mohandas, N., *et al.* (1998). The FERM domain: A unique module involved in the linkage of cytoplasmic proteins to the membrane. *Trends Biochem. Sci.* **23:** 281–282.

Coluccio, L. M. (1997). Myosin I. *Am. J. Physiol.* **273:** C347–359.

Cope, M. J. T. V., Whisstock, J., Rayment, I., and Kendrick-Jones, J. (1996). Conservation within the myosin motor domain: Implications for structure and function. *Structure* **4:** 969–987.

Felsenstein, J. (1993). PHYLIP (Phylogeny Inference Package), version 3.6, University of Washington, Seattle.

García-Añoveros, J., Derfler, B., Neville-Golden, J., Hyman, B. T., and Corey, D. P. (1997). BNaC1 and BNaC2 constitute a new family of human neuronal sodium channels related to degenerins and epithelial sodium channels. *Proc. Natl. Acad. Sci. USA* **94:** 1459–1464.

Geisterfer-Lowrance, A. A., Kass, S., Tanigawa, G., Vosberg, H. P., McKenna, W., Seidman, C. E., and Seidman, J. G. (1990). A molecular basis for familial hypertrophic cardiomyopathy: A beta cardiac myosin heavy chain gene missense mutation. *Cell* **62:** 999–1006.

Gibson, F., Walsh, J., Mburu, P., Varela, A., Brown, K. A., Antonio, M., Beisel, K. W., Steel, K. P., and Brown, S. D. M. (1995). A type VII myosin encoded by the mouse deafness gene *Shaker-1*. *Nature* **374:** 62–64.

Halbhuber, K. J., Schulze, M., Rhode, H., Bublitz, R., Feuerstein, H., Walter, M., Linss, W., Meyer, H. W., and Horn, A. (1994). Is the brush border membrane of the intestinal mucosa a generator of "chymosomes"? *Cell. Mol. Biol.* **40:** 1077.

Hasson, T. (1999). Sensing a function for myosin-VIIa. *Curr. Biol.* **9:** R838–R841.

Hasson, T., Gillespie, P. G., Garcia, J. A., MacDonald, R. B., Zhao, Y., Yee, A. G., Mooseker, M. S., and Corey, D. P. (1997). Unconventional myosins in inner-ear sensory epithelia. *J. Cell Biol.* **137:** 1287–1307.

Hasson, T., Heintzelman, M. B., Santos-Sacchi, J., Corey, D. P., and Mooseker, M. S. (1995). Expression in cochlea and retina of myosin-VIIa, the gene product defective in Usher syndrome type 1B. *Proc. Natl. Acad. Sci. USA* **92:** 9815–9819.

Hasson, T., and Mooseker, M. S. (1994). Porcine myosin-VI: Characterization of a new mammalian unconventional myosin. *J. Cell Biol.* **127:** 425–440.

Hasson, T., Skowron, J. F., Gilbert, D. J., Avraham, K. B., Perry, W. L., Bement, W. M., Anderson, B. L., Sherr, E. H., Chen, Z.-Y., Greene, L. A., Ward, D. C., Corey, D. P., Mooseker, M. S., Copeland, N. G., and Jenkins, N. A. (1996). Mapping of unconventional myosins in mouse and human. *Genomics* **36:** 431–439.

Heintzelman, M. B., Hasson, T., and Mooseker, M. S. (1994). Multiple unconventional myosin domains of the intestinal brush border cytoskeleton. *J. Cell Sci.* **107:** 3535–3543.

Hodge, T., and Cope, M. J. (2000). A myosin family tree. *J. Cell Sci.* **113:** 3353–3354.

Kuriyan, J., and Cowburn, D. (1997). Modular peptide recognition domains in eukaryotic signaling. *Annu. Rev. Biophys. Biomol. Struct.* **26:** 259–288.

Liang, Y., Wang, A., Belyantseva, I. A., Anderson, D. W., Probst, F. J., Barber, T. D., Miller, W., Touchman, J. W., Jin, L., Sullivan, S. L., Sellers, J. R., Camper, S. A., Lloyd, R. V., Kachar, B., Friedman, T. B., and Fridell, R. A. (1999). Characterization of the human and mouse unconventional myosin XV genes responsible for hereditary deafness DFNB3 and Shaker 2. *Genomics* **61:** 243–258.

Liu, X., Udovichenko, I. P., Brown, S. D., Steel, K. P., and Williams, D. S. (1999). Myosin VIIa participates in opsin transport through the photoreceptor cilium. *J. Neurosci.* **19:** 6267–6274.

Mao, N. C., Steingrimsson, E., DuHadaway, J., Wasserman, W., Ruiz, J. C., Copeland, N. G., Jenkins, N. A., and Prendergast, G. C. (1999) The murine Bin1 gene functions early in myogenesis and defines a new region of synteny between mouse chromosome 18 and human chromosome 2. *Genomics* **56:** 51–58.

Mburu, P., Liu, X. Z., Walsh, J., Saw, D., Jr., Cope, M. J., Gibson, F., Kendrick-Jones, J., Steel, K. P., and Brown, S. D. (1997). Mutation analysis of the mouse myosin VIIA deafness gene. *Genes Funct.* **1:** 191–203.

Mercer, J. A., Seperack, P. K., Strobel, M. C., Copeland, N. G., and Jenkins, N. A. (1991). Novel myosin heavy chain encoded by murine dilute coat colour locus. *Nature* **349:** 709–713.

Misch, D. W., Giebel, P. E., and Faust, R. G. (1980). Intestinal microvilli: Responses to feeding and fasting. *Eur. J. Cell Biol.* **21:** 269.

Mooseker, M. S., Wolenski, J. S., Coleman, T. R., Hayden, S. M., Cheney, R. C., Espreafico, E., Heintzelman, M. B., and Peterson, M. D. (1991).Structural and functional dissection of a membrane-bound mechanoenzyme: Brush border myosin I. *In* "Current Topics in Membranes: Ordering the Membrane Cytoskeleton Trilayer" (M. S. Mooseker and J. S. Morrow, Eds.), p. 31, Academic Press, Orlando, FL.

Narasimhulu, S. B., and Reddy, A. S. (1998). Characterization of microtubule binding domains in the *Arabidopsis* kinesin-like calmodulin binding protein. *Plant Cell* **10:** 957–965.

Oliver, T. N., Berg, J. S., and Cheney, R. E. (1999). Tails of unconventional myosins. *CMLS Cell. Mol. Life Sci.* **56:** 243–257.

Pastural, E., Barrat, F. J., Dufourcq-Lagelouse, R., Certain, S., Sanal, O., Jabado, N., Seger, R., Griscelli, C., Fischer, A., and de Saint Basile, G. (1997). Griscelli disease maps to chromosome 15q21 and is associated with mutations in the myosin-Va gene. *Nat. Genet.* **16:** 289–292.

Probst, F. J., Fridell, R. A., Raphael, Y., Saunders, T. L., Wang, A., Liang, Y., Morell, R. J., Touchman, J. W., Lyons, R. H., Noben-Trauth, K., Friedman, T. B., and Camper, S. A. (1998). Correction

of deafness in shaker-2 mice by an unconventional myosin in a BAC transgene. *Science* **280:** 1444–1447.

Richardson, G. P., Forge, A., Kros, C. J., Fleming, J., Brown, S. D., and Steel, K. P. (1997). Myosin VIIA is required for aminoglycoside accumulation in cochlear hair cells. *J. Neurosci.* **17:** 9506–9519.

Skowron, J. F., Bement, W. M., and Mooseker, M. S. (1998). Human brush border myosin-I and myosin-Ic expression in human intestine and Caco-2BBe cells. *Cell Motil. Cytoskeleton* **41:** 308–324.

Solc, C. K., Derfler, B. H., Duyk, G. M., and Corey, D. P. (1994). Molecular cloning of myosins from the bullfrog saccular macula: A candidate for the adaptation motor. *Auditory Neurosci.* **1:** 63–75.

Strong, T. V., Tagle, D. A., Valdes, J. M., Elmer, L. W., Boehm, K., Swaroop, M., Kaatz, K. W., Collins, F. S., and Albin, R. L. (1993). Widespread expression of the human and rat Huntington's disease gene in brain and nonneural tissues. *Nat. Genet.* **5:** 259–265.

Thompson, J. D., Gibson, T. J., Plewniak, F., Jeanmougin, F., and Higgins, D. G. (1997). The CLUSTAL_X windows interface: Flexible strategies for multiple sequence alignment aided by quality analysis tools. *Nucleic Acids Res.* **25:** 4876–4882.

Titus, M. A. (1999). A class VII unconventional myosin is required for phagocytosis. *Curr. Biol.* **9:** 1297–1303.

Wang, A., Liang, Y., Firdell, R. A., Probst, F. J., Wilcox, E. R., Touchman, J. W., Morton, C. C., Morell, R. J., Noben-Trauth, K., Camper, S. A., and Friedman, T. B. (1998). Association of unconventional myosin MYO15 mutations with human nonsyndromic deafness DFNB3. *Science* **280:** 1447–1451.

Wasserman, R. H., and Fullmer, C. S. (1995). Vitamin D and intestinal calcium transport: Facts, speculations and hypotheses. *J. Nutr.* **125:** 1971S–1979S.

Weil, D., Blanchard, S., Kaplan, J., Guilford, P., Gibson, F., Walsh, J., Mburu, P., Varela, A., Levilliers, J., and Weston, M. D. (1995). Defective myosin VIIA gene responsible for Usher syndrome type IB. *Nature* **374:** 60–61.

Weil, D., Levy, G., Sahly, I., Levi-Acobas, F., Blanchard, S., El-Amraoui, A., Crozet, F., Philippe, H., Abitbol, M., and Petit, C. (1996). Human myosin VIIA responsible for the Usher 1B syndrome: A predicted membrane-associated motor protein expressed in developing sensory epithelia. *Proc. Natl. Acad. Sci. USA* **93:** 3232–3237.

White, J. V., Stultz, C. M., and Smith T. F. (1994) Protein classification by stochastic modeling and optimal filtering of amino-acid sequences. *Math. Biosci.* **119:** 35–75.

Wu, X., Jung, G., and Hammer, J. A. (2000). Functions of unconventional myosins. *Curr. Opin. Cell Biol.* **12:** 42–51.

Xu, P., Mitchelhill, K. I., Kobe, B., Kemp, B. E., and Zot, H. G. (1997). The myosin-I-binding protein Acan125 binds the SH3 domain and belongs to the superfamily of leucine-rich repeat proteins. *Proc. Natl. Acad. Sci. USA* **94:** 3685–3690.